Electronic Supplementary Material (ESI) for Nanoscale.

Supporting Information

C-CoP hollow microporous nanocages derived from Prussian blue analogue: high-performance bifunctional electrocatalyst for overall water splitting

Wanping Li[a], Gao Cheng[a], Ming Sun[a], Zhaoxuan Wu[b], Guanliang Liu[a], Dangsheng Su[b], Bang Lan [a, c], Shixin Mai[a], Liya Chen[a], Lin Yu*[,a]

[a]Key Laboratory of Clean Chemistry Technology of Guangdong Regaular Higher Education Institutions, School of Chemical Engineering and Light Industry, Guangdong University of Technology, Guangzhou 510006, P. R. China

[b]Dalian National Laboratory for Clean Energy (DNL), Dalian Institute of Chemical Physics, Chinese Academy of Sciences, Dalian 116023, P. R. China.

[c]GuangDong MeiZhou Quality & Metrology Supervision and Testing Institution, Meizhou, 514072, P. R. China.

E-mail: gych@gdut.edu.cn (Lin Yu).

Experimental

Materials

$Co(CH_3COO)_2{\cdot}H_2O$ and $NaH_2PO_2{\cdot}H_2O$ were purchased by Guangzhou Chemical Reagent Factory. (China). $K_3[Co(CN)_6]$ and polyvinylpyrrolidone (PVP, K54-K65) were bought from Energy Chemical. (China). All chemical reagents were used as received without further purification.

Catalysts preparation

Preparation of PBA-Co

Prussian blue analogs-Co nanocages (PBA-Co) were synthesized according to a facile solution method. In a typical procedure, 3 g polyvinylpyrrolidone and 0.4 mmol $K_3[Co(CN)_6]$ were dissolved in water to form solution A. 0.75mmol $Co(CH_3COO)_2{\cdot}H_2O$ was dissolved in another 100mL water to form solution B. Subsequently, solution B was slowly added into solution A with vigorous stirring. The mixture was then placed in ambient for 20 h. The obtained pink product was separated by centrifugation and washed several times with distilled water and absolute ethanol, and finally dried in a vacuum oven at 60 °C overnight.

Preparation of C-Co_3O_4

To prepare C coated Co_3O_4 hollow porous nanocages (C-Co_3O_4), the PBA precursors was annealed in air at 350 ºC for 0.5 h with a heating rate of 1 °C min^{-1}.

Preparation of C-CoP

The as-synthesized C-Co_3O_4 and $NaH_2PO_2{\cdot}H_2O$ were placed two porcelain boat separately, and $NaH_2PO_2{\cdot}H_2O$ was at the upstream side of the tube furnace. The molar ratio for Co to P was 1:6/12/18. The samples were calcined at 320 °C for 1 h with a heating speed of 1 °C min^{-1} in Ar flow., and then naturally cooled to ambient temperature. The resulted powders were named as C-CoP-1/6, C-CoP-1/12 and C-CoP-1/18 respectively.

Moreover, as a further verification test, the less C coated CoP （C-CoP-1/12(L)）was synthesized in a similar way as that of C-C-CoP-1/12 by increasing the oxidation temperature and time to 400 ºC and 2 h.

Materials characterization

Powder X-ray diffraction patterns (XRD) were collected on a PANalytical X-ray Diffractometer (X'Pert3 Powder) equipped with a Cu Kα radiation. The field emission scanning electron microscope (FE-SEM) images were performed on a Hitachi SU8010 instrument. Transmission electron microscopy (TEM) images and Select area electron diffraction (SAED) pattern were acquired on a JEOL JEM2100 with an accelerating voltage of 200 kV. Energy-dispersive X-ray Spectrometer elemental mapping (EDX-mapping) images were available from FEI titan themis 200 TEM. X-ray photoelectron spectroscopy (XPS) were recorded on a Thermo Fisher Escalab 250Xi spectrometer. The Brunauer-Emmett-Teller (BET) nitrogen physisorption experiments were carried out on a Micromeritics ASAP 2020. Element content was measured on an Agilent ICPOES730.

Electrochemical measurements

The electrochemical data was collected in 1.0 M KOH by using a ZAHNER ZENNIUM/IM6 electrochemical workstation. The electrochemical test for HER and OER was performed in a standard three-electrode system using a sample-coated glassy carbon as a working electrode, an Ag/AgCl (3.5 M KCl) as a reference electrode, a graphite rod as a counter electrode in HER, a Pt foil as a counter electrode in OER. To fabricate the working electrode, the catalyst ink was prepared by ultrasonication of the mixture of 5 mg of catalyst, 50 μL of 5 wt % Nafion, 475 μL of water and 475 μL of ethanol, then 12 μL of the ink was drop-casted onto the glassy carbon L-typed disk electrode with a diameter of 5 mm and dried at room temperature with a mass loading of 0.306 mg cm^{-2}. The scan rate of Polarization curves (LSVs) were 2 mV s^{-1} at 25 °C. The measured potentials in this work were converted to RHE through the following equation: $E_{RHE} = E_{Ag/AgCl} + 0.059pH + E^0_{Ag/AgCl}$, and all of potentials in the LSV polarization curves were not iR-corrected. Electrochemical impedance spectroscopy (EIS) measurement was carried out at different overpotentials in the frequency range of 100 kHz to 100 mHz with a 5 mV ac amplitude. According to Polarization curves, the Tafel plots were plotted by fitting to the Tafel equation: $\eta = a + b \log j$ (where η is the overpotential, a is the intercept relative to the exchange current density (j_0), j is the current density and b is the Tafel slope. The long-term stability was tested by a galvanostatic method at 10 mA cm^{-2} current density. The double layer capacitance (C_{dl}) was calculated to estimate the electrochemical active surface areas (ECSAs) of catalysts, because it is linearly proportional to the ECSAs. The C_{dl} was determined by using the cyclic voltammograms (CVs) recorded at non-Faradaic potentials (1.10-1.15 V vs. RHE for OER, 0.10-0.15 V vs. RHE for HER) at different scan rates.

To evaluate the practical application of C-CoP-1/12 in water electrolysis reaction, the catalyst was coated on carbon paper (1 cm × 1cm) with a mass loading of ~1.528 mg cm^{-2} and used as cathode and anode directly. To prepared electrode materials, 1 mg of Polyvinylidene fluoride was dispersed in the 0.5 mL of N-Methyl pyrrolidone, then added 9 mg of the catalyst and ground evenly. The LSV curves were recorded in 1.0 M KOH with a scan rate of 2 mV s^{-1}. The long-term durability was assessed by the galvanostatic method.

DFT computation

The free energy calculations were performed based on the density functional theory (DFT) by using the method encoded in the Vienna ab-initio simulation package (VASP).[1, 2] The interactions between valence electrons and ion cores were treated by Blöchl's all-electron-like Projector Augmented Wave (PAW) method.[3, 4] The generalized gradient approximation with Perdew-Burke-Ernzerhof (GGA-PBE) functional was selected to describe the exchange and correlation effects.[5] An energy cutoff of 400 eV was set. The energy that converged to 10^{-6} eV per atom and the force that converged to 10^{-2} eV $Å^{-1}$ were chosen as the convergence criteria of geometry optimization, respectively. Brillouin zone integration was approximated by a sum over special selected k-points with a 3×3×1 Monkhorst–Pack grids.[6] The DFT-D3 force-field approach was used to consider the van der Waals (vdW) interaction. Due to the existence of the magnetic atoms Co, spin polarization was considered throughout the calculations. All the calculations are performed on (011) surface of CoP and Co_2P. A four layers and 2×1 supercell were built for models. During the structural optimization, the bottom two layers were fixed, while the positions of other two atomic layers were allowed to relax. A vacuum space as large as 15 Å was used along the z direction normal to the surface to avoid periodic interactions. The Co-P bridge site was selected as the adsorption site in the calculations. The free energy change for H* adsorptions ($^{\Delta G_{H*}}$) were calculated as follows:

$$\Delta G_{H*} = \Delta E_{H*} + \Delta E_{ZPE} - T\Delta S$$

Where $^{\Delta E_{H*}}$ is the adsorption energy of H species, T is the system temperature (298.15 K), $^{\Delta E_{ZPE}}$ and ΔS are the energy change in zero point energy and entropy, respectively. The harmonic vibrational frequency calculations were performed to obtain the Zero Point Energy (ZPE) corrections[7].

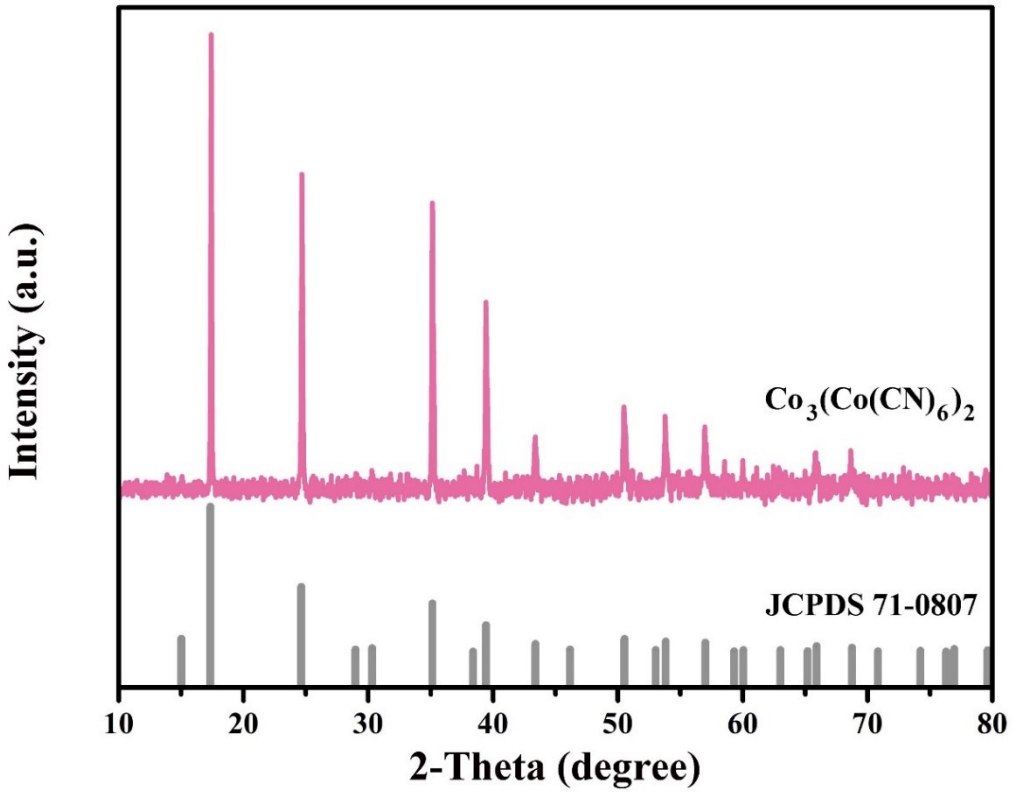

Figure S1. XRD pattern of PBA-Co.

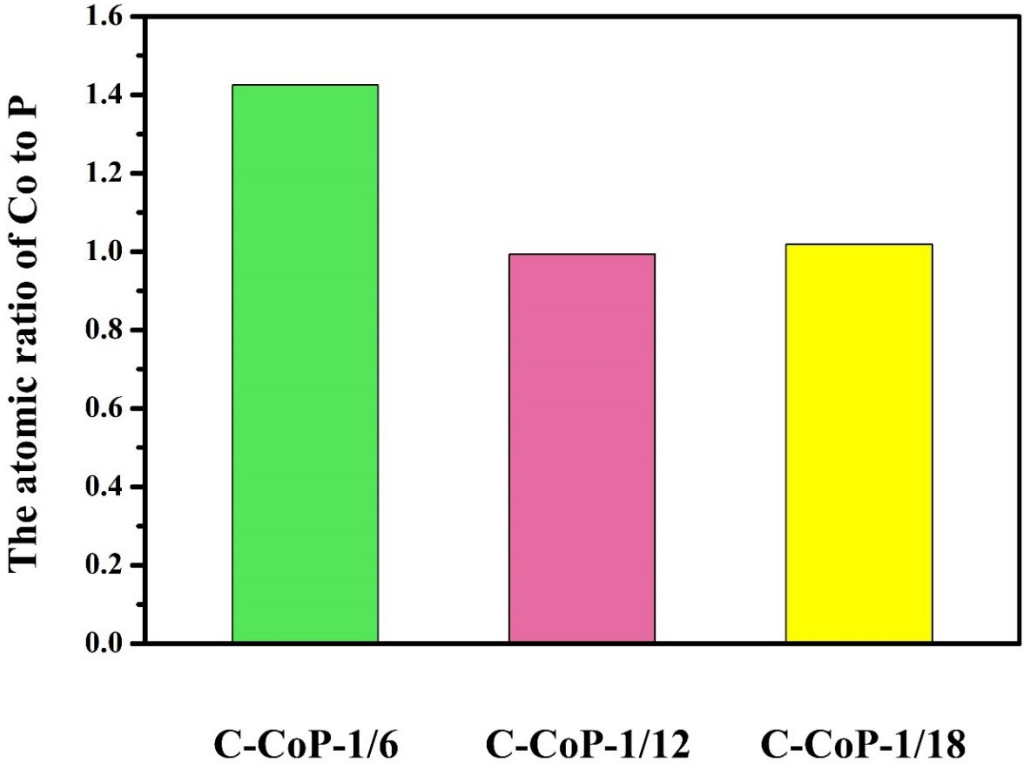

Figure S2. The actual molar ratio of Co and P for C-CoP-1/6, C-CoP-1/12 and C-CoP-1/18 acquired from ICP-OES test result.

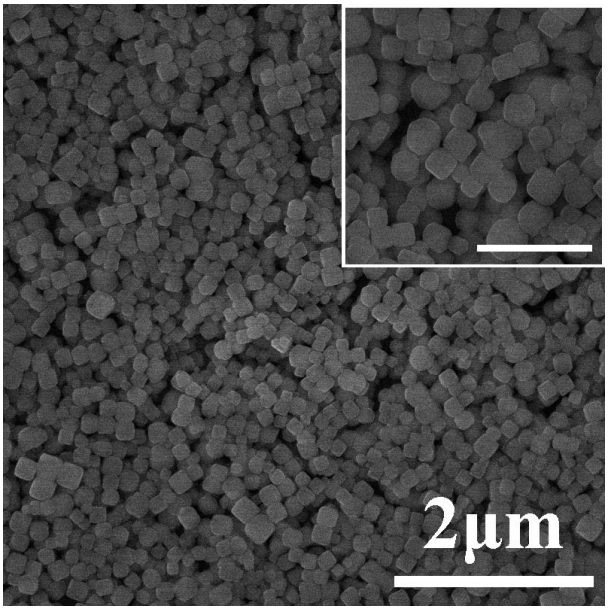

Figure S3. FESEM images of PBA-Co, and the ruler of inner images is 300 nm.

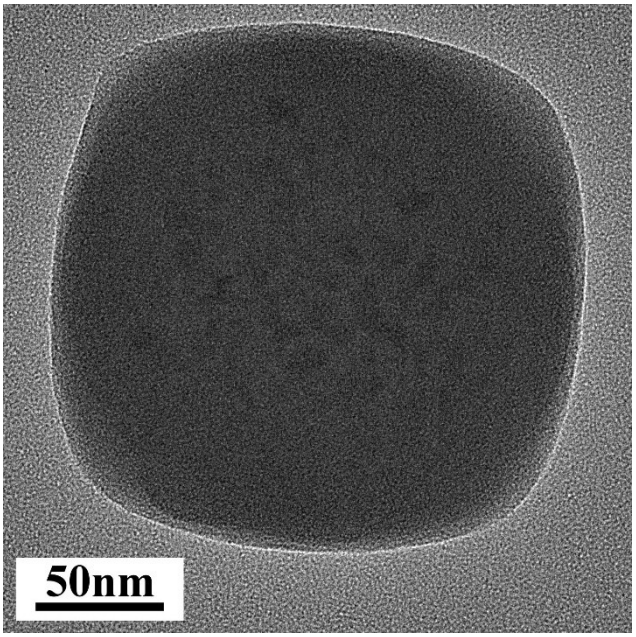

Figure S4. TEM image of PBA-Co.

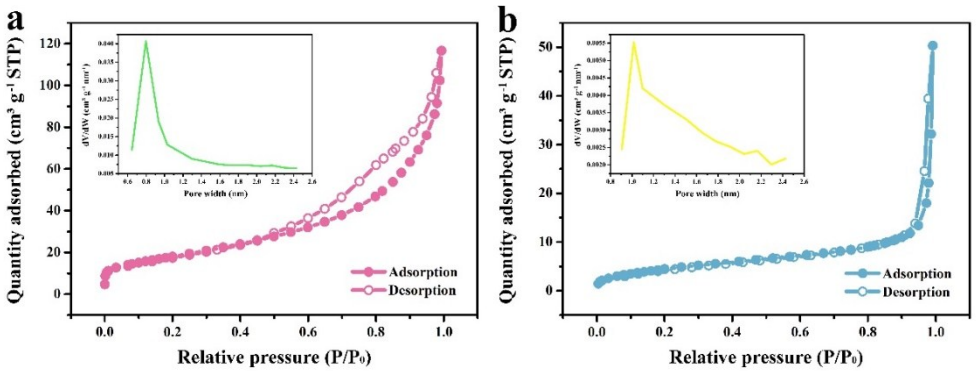

Figure S5. The typical N_2 adsorption-desorption isotherms and HK differential pore volume plot (inset) of the C-Co_3O_4 (a) and C-CoP-1/12 (b).

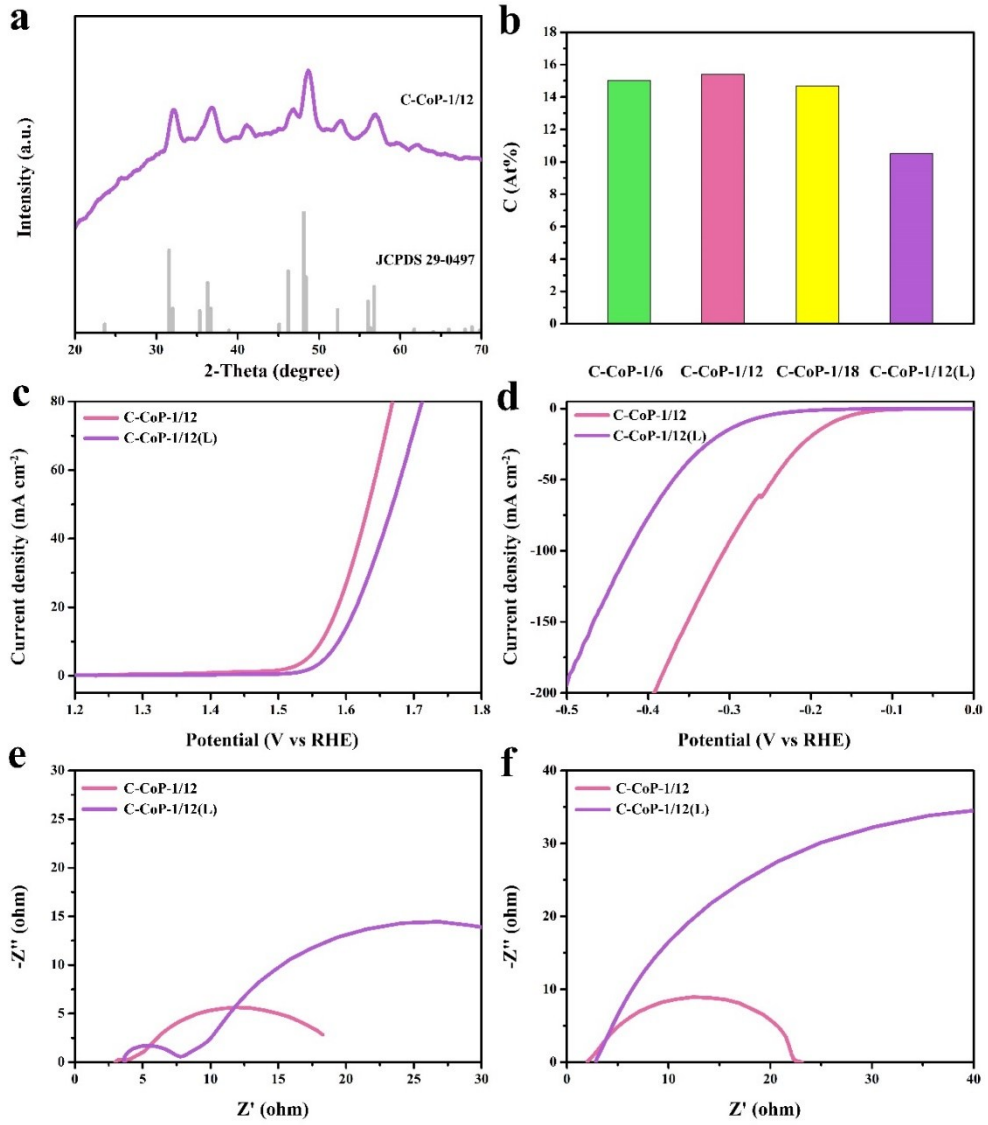

Figure S6. XRD patterns of C-CoP-1/12(L) (a); The C content of as prepared catalysts acquired from EDX elemental analysis result (b); LSV polarization curves for OER (c) and HER (d); Nyquist plots for OER (e) and HER (f). (Red and purple represent C-CoP-1/12 and C-CoP-1/12(L) respectively.)

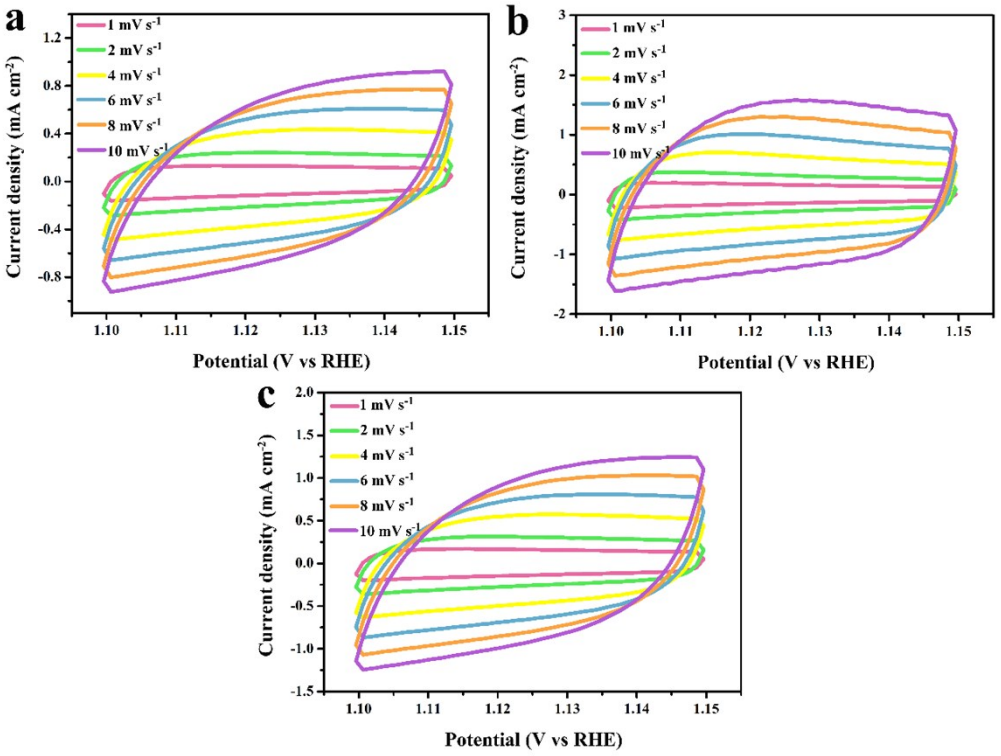

Figure S7. CV curves of C-CoP-1/6 (a), C-CoP-1/12 (b) and C-CoP-1/18 (c) measured at different scan rates from 1 to 10 mV s^{-1} for OER.

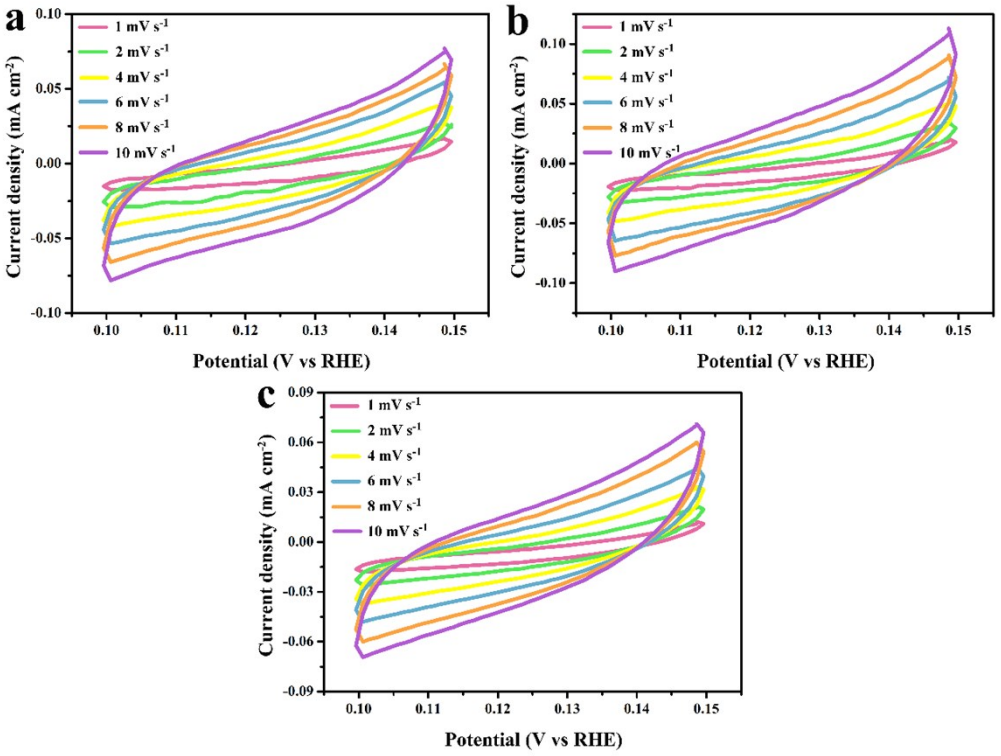

Figure S8. CV curves of C-CoP-1/6 (a), C-CoP-1/12 (b) and C-CoP-1/18 (c) measured at different scan rates from 1 to 10 mV s^{-1} for HER.

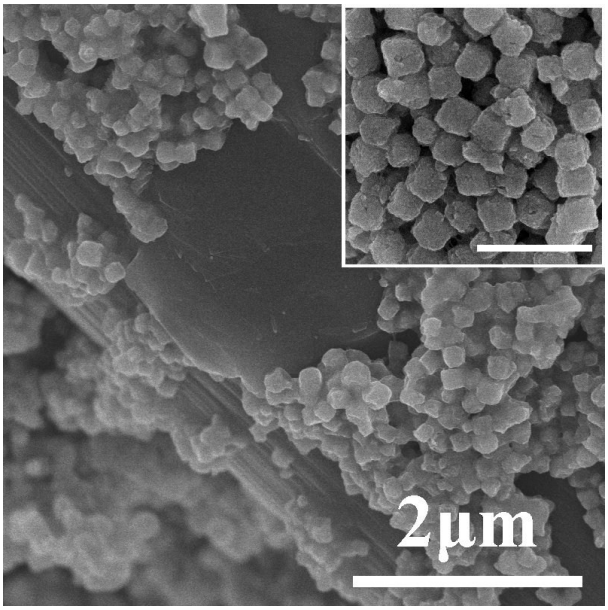

Figure S9. SEM images of C-CoP-1/12(CP), and the ruler of inner images is 300 nm.

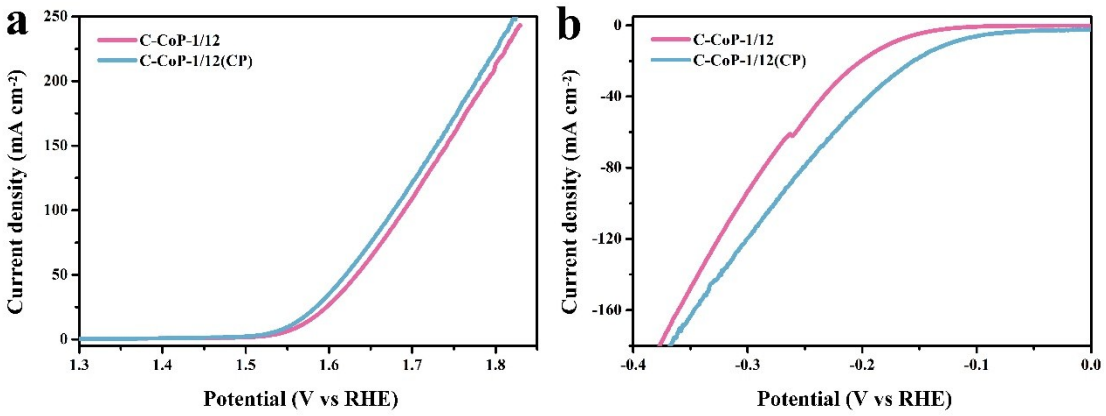

Figure S10. LSV polarization curves for OER (a) and HER (b) over C-CoP-1/12 and C-CoP-1/12(CP).

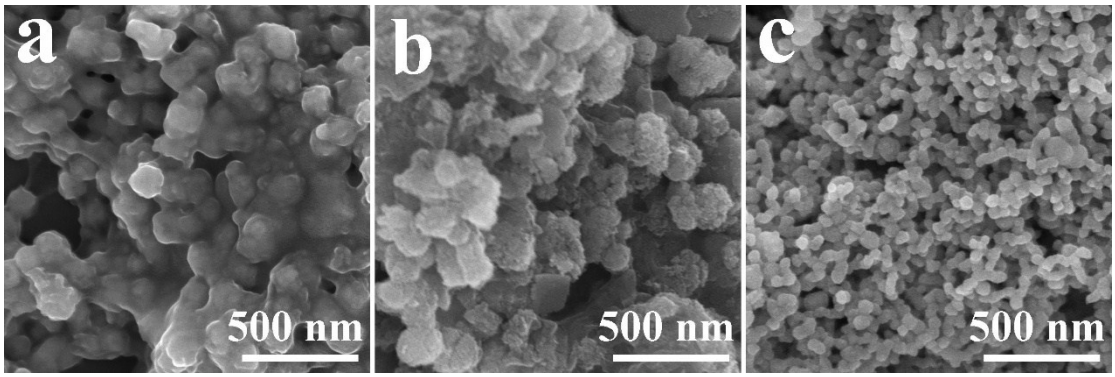

Figure S11. FESEM images of C-CoP-1/12 ink before test (a), after OER stability test (b) and after HER stability test (c).

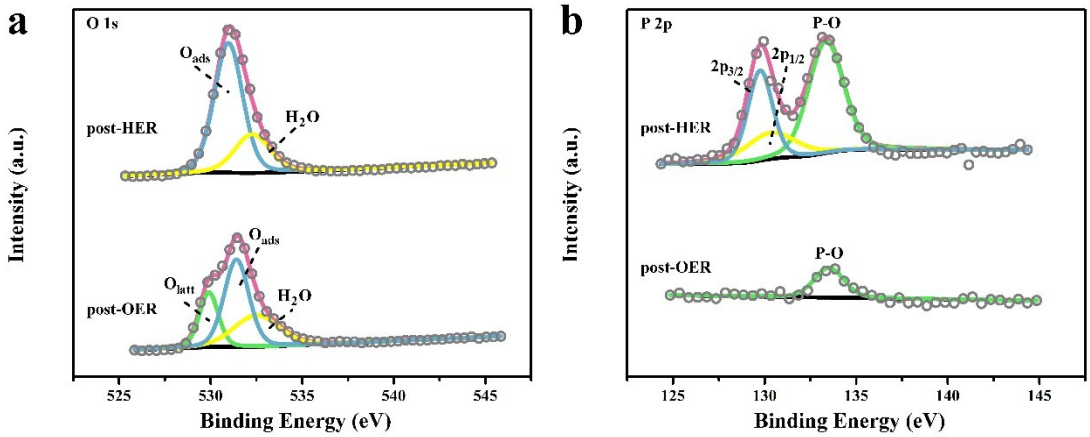

Figure S12. High-resolution XPS spectra of C-CoP-1/12 after 24h durability test: O 1s (a), P 2p (b).

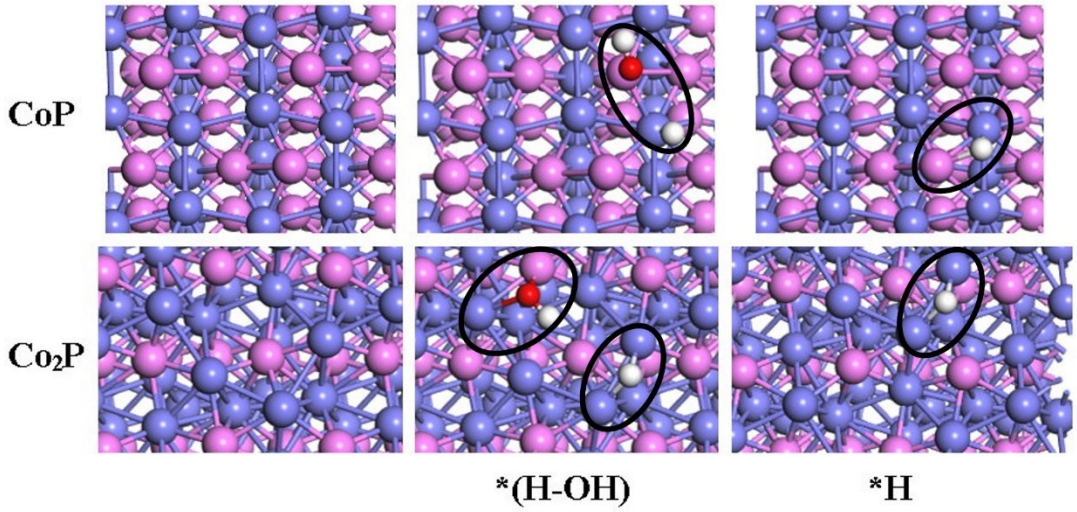

Figure S13. Crystal structure models of CoP and Co_2P; The configuration of intermediates adsorbed on the CoP and Co_2P during alkaline HER reaction process, respectively. (Blue, purple, red and white ball represent Co, P, C and H atom, respectively.).

Catalysts	**Category and Loading**	**OER performance in 1.0 M KOH**	**HER performance in 1.0 M KOH**	**overall water-splitting performance**	**Reference**
		Overpotential η (@ j10 / mV)	**Overpotential η (@ j10 / mV)**	**Potential η (@ j10 / mV)**	
C-CoP-1/12	**Powder; 0.306 mg/cm^2**	**333**	**174**	——	**This work**
	Integrate; 1.528 mg/cm^2	**321**	**123**	**1.650**	
CP@FeP	Integrate; 0.7 mg/cm^2	350	——	——	1[8]
Ni_2P nanowires	Powder; 0.10 mg/cm^2	400	——	——	2[9]
CoP NR/C	Powder; 0.71 mg/cm^2	350	——	——	3[10]
sandwich-like CoP/C	Powder; 0.36 mg/cm^2	330	——	——	4[11]
CoP/CC	Integrate; 0.92 mg/cm^2	——	209	——	5[12]
FeP NAs/CC	Integrate; 1.5 mg/cm^2	——	218	——	6[13]
CFP-FeP HNA	Integrate 3.8 mg/cm^2	——	181	——	7[14]
CoP Hollow Polyhedra	Powder; 0.102 mg/cm^2	400	159	——	8[15]
CoP/rGO-400	Powder; 0.28 mg/cm^2	340	150	1.700	9[16]
Ni-P NA/NF	Integrate; 31.5 mg/cm^2	350	148	1.690	10[17]
Co_2P/Co-foil	Integrate; ——	319	154	1.710	11[18]
NiMoN-550 nanotubes	Powder; 3.50 mg/cm^2	295	89	1.596	12[19]

Ni-Fe-MoN NTs	Powder; 3.50 mg/cm^2	228	55	1.513	13[20]
Co_3C-NB	Powder; 0.353 mg/cm^2	358(0.1M KOH)	154		14[21]

Table S1. Recent published phosphide catalysts and their OER, HER and Overall water splitting catalytic activity.

1. G. Kresse and J. Furthmuller, *Computational Materials Science*, 1996, **6**, 15-50.
2. G. Kresse and J. Furthmuller, *Physical Review B*, 1996, **54**, 11169-11186.
3. P. E. Blochl, *Physical Review B*, 1994, **50**, 17953-17979.
4. G. Kresse and D. Joubert, *Physical Review B*, 1999, **59**, 1758-1775.
5. J. P. Perdew, K. Burke and M. Ernzerhof, *Physical Review Letters*, 1996, **77**, 3865-3868.
6. H. J. Monkhorst and J. D. Pack, *Physical Review B*, 1976, **13**, 5188-5192.
7. H. Cao, Y. Xie, H. Wang, F. Xiao, A. Wu, L. Li, Z. Xu, N. Xiong and K. Pan, *Electrochimica Acta*, 2018, **259**, 830-840.
8. D. Xiong, X. Wang, W. Li and L. Liu, *Chemical communications*, 2016, **52**, 8711-8714.
9. A. Han, H. Chen, Z. Sun, J. Xu and P. Du, *Chemical communications*, 2015, **51**, 11626-11629.
10. J. Chang, Y. Xiao, M. Xiao, J. Ge, C. Liu and W. Xing, *ACS Catalysis*, 2015, **5**, 6874-6878.
11. Y. Bai, H. Zhang, Y. Feng, L. Fang and Y. Wang, *Journal of Materials Chemistry A*, 2016, **4**, 9072-9079.
12. J. Tian, Q. Liu, A. M. Asiri and X. Sun, *Journal of the American Chemical Society*, 2014, **136**, 7587-7590.
13. Y. Liang, Q. Liu, A. M. Asiri, X. Sun and Y. Luo, *ACS Catalysis*, 2014, **4**, 4065-4069.
14. C. Lv, Z. Peng, Y. Zhao, Z. Huang and C. Zhang, *Journal of Materials Chemistry A*, 2016, **4**, 1454-1460.
15. M. Liu and J. Li, *ACS applied materials & interfaces*, 2016, **8**, 2158-2165.
16. L. Jiao, Y. X. Zhou and H. L. Jiang, *Chem Sci*, 2016, **7**, 1690-1695.
17. J. Xiao, Q. Lv, Y. Zhang, Z. Zhang and S. Wang, *RSC Advances*, 2016, **6**, 107859-107864.
18. C.-Z. Yuan, S.-L. Zhong, Y.-F. Jiang, Z. K. Yang, Z.-W. Zhao, S.-J. Zhao, N. Jiang and A.-W. Xu, *Journal of Materials Chemistry A*, 2017, **5**, 10561-10566.
19. Z. Yin, Y. Sun, C. Zhu, C. Li, X. Zhang and Y. Chen, *Journal of Materials Chemistry A*, 2017, **5**, 13648-13658.
20. C. Zhu, Z. Yin, W. Lai, Y. Sun, L. Liu, X. Zhang, Y. Chen and S.-L. Chou, *Advanced Energy Materials*, 2018, **8**, 1802327.
21. X. Ma, K. Li, X. Zhang, B. Wei, H. Yang, L. Liu, M. Zhang, X. Zhang and Y. Chen, *Journal of Materials Chemistry A*, 2019, **7**, 14904-14915.